Erschienen in: Advanced Materials ; 17 (2005), 12. - S. 1461-1465
https://dx.doi.org/10.1002/adma.200401957

Polymer-Directed Formation of Unusual $CaCO_3$ Pancakes with Controlled Surface Structures**

By *Shao-Feng Chen*, *Shu-Hong Yu*,* *Tong-Xin Wang*, *Jun Jiang*, *Helmut Cölfen*,* *Bing Hu*, and *Bo Yu*

Biominerals in natural organisms have attracted increasing interest because of their important and unique optical and mechanical properties, induced by the unique morphologies and arrangements of micro-biomineral crystals.[1] For example, the optical properties of pearls and the mechanical properties of teeth and bone have many advantages over corresponding synthetic crystals.[2] Consequently, the bio-inspired synthesis of crystals with complex forms that mimic natural biominerals has became a hot area of research.[3] Among many examples, a complex growth mechanism for the growth of fluoroapatite in gelatin gels was first reported in detail by Kniep and Busch.[4] The synthesis of biomimetic arrays of oriented helical ZnO nanorods and columns using seeds to control the nucleation and citrate anions to control the morphology[5] and the synthesis of pancake-like ZnO structures controlled by the block copolymer poly(ethylene oxide)–*block*–(polystyrene sulfonic acid) have been reported.[6] Recently, we demonstrated the formation of very long helices by the tectonic arrangement of $BaCO_3$ nanocrystals induced by a racemic block copolymer.[7] Kotov et al. demonstrated the self-assembly of a layered clay–polyelectrolyte structure with an interesting analogy to the biomineral nacre.[8] Such layered structures are interesting as, for example, they can show improved mechanical properties, as in the case of $CaCO_3$-based nacre with interspaced soft chitin/protein layers. Such layered structures, which exist in seashells, are usually not easily attainable.[9] Exploration of a rational way to mimic complex, oriented nanostructures like seashells, preferably via a self-assembly mechanism, remains a significant challenge.

[*] Prof. S. H. Yu, S. F. Chen, J. Jiang, B. Hu, B. Yu
Division of Nanomaterials and Chemistry, Hefei National Laboratory for Physical Sciences at Microscale, Structure Research Laboratory of CAS, Department of Materials Science and Engineering, Department of Chemistry
University of Science and Technology of China
Hefei, Anhui 230026 (P.R.China)
E-mail: shyu@ustc.edu.cn
Dr. H. Cölfen, Dr. T. X. Wang
Department of Colloid Chemistry
Max Planck Institute of Colloids and Interfaces
MPI Research Campus Golm, D-14424 Potsdam (Germany)
E-mail: coelfen@mpikg-golm.mpg.de

[**] S. H. Y. acknowledges special funding support from the Centurial Program of the Chinese Academy of Sciences, the National Natural Science Foundation of China (NSFC, Nos. 20325104, 20321101, 50372065), and the Scientific Research Foundation for the Returned Overseas Chinese Scholars, State Education Ministry. H. C. and T. X. W. thank the Max Planck Society for funding. Supporting Information is available online from Wiley InterScience or from the authors.

$CaCO_3$ is a typical biomineral found in organisms and is abundant in Nature. It has found significant industrial use as a filler in plastic, paper, and in decorative paints.[10] Therefore, biomimetic synthesis and shape-control of $CaCO_3$ crystals with complex forms have become recent foci of research, and many complex morphologies have been reported.[3g,11] However, in most cases, the additive–crystal interaction could not be revealed, and, up until now, mechanistic understanding of additive-controlled mineralization is still lacking. Weiner and Traub suggested an epitaxial model for aragonite formation in nacre with a distinct ●●1 orientation,[12,13] which appeared to explain biomineral formation well. This has inspired many studies—especially those in which monolayers are used as crystallization templates.[14]

Herein, we present the double-hydrophilic block copolymer (DHBC)[3h,15]-directed self-assembly of unusual calcite pancakes with controlled surface structures, using the macrocycle-coupled block copolymer, poly(ethylene glycol)–*b*–poly(1,4,7,1●,13,16-hexaazacyclooctadecan ethylene imine), macrocycle (PEG–*b*–hexacyclen), as a crystal modifier (weight-average molecular weight, M_w, of PEG = 5●●● g mol^{-1}; M_w of macrocycle = 5●● g mol^{-1}; Scheme 1).

This polymer is special, in that its functional block is rigid and thus shape persistent, and can be complexing or cationic under the applied conditions, thus making it a good candidate for controlled interaction with crystal surfaces. Macrocycles, including crown ethers and hexacyclens, have been investigated extensively for many years due to their tunable internal cavities and strong interaction with neutral molecules, cations, and anions, through host–guest interactions.[16] The polymer was synthesized according to a previously reported procedure.[17] Room-temperature mineralization of $CaCO_3$ was performed using a slow gas-diffusion procedure, as described elsewhere.[18]

The mineralization reaction under ambient conditions, using different concentrations of the polymer, resulted in the formation of calcite crystals, as confirmed by the X-ray diffraction (XRD) patterns shown in Figure 1.

Figure 2 presents typical scanning electron microscopy (SEM) images of the self-stacked calcite "pancakes" obtained after 2 weeks of mineralization. The lower-magnification image (Fig. 2a) shows the piled $CaCO_3$ crystals, indicating that all the $CaCO_3$ pancakes are rather round and their diameters range from 26 to 29 μm with a thickness of about 8 μm (Figs. 2b,c). These self-assembled pancakes made of stacked multilayers show distant structural similarities to the layered structures of nacre in *Haliotis rufescens* (red abalone).[5b] To the best of our knowledge, such multilayer pancake calcite structures have not been synthesized previously.

It is interesting to note that the diameters of the outer layers in a given stack are slightly smaller than those of the central layers (Figs. 2b,c). The magnified SEM image in Figure 2d shows that the thickness of each layer ranges from 1●● to 35● nm, and many thicker layers (with thicknesses of about 28●–35● nm) are split into two or more thinner layers (with thicknesses of about 1●●–2●● nm). Closer examination

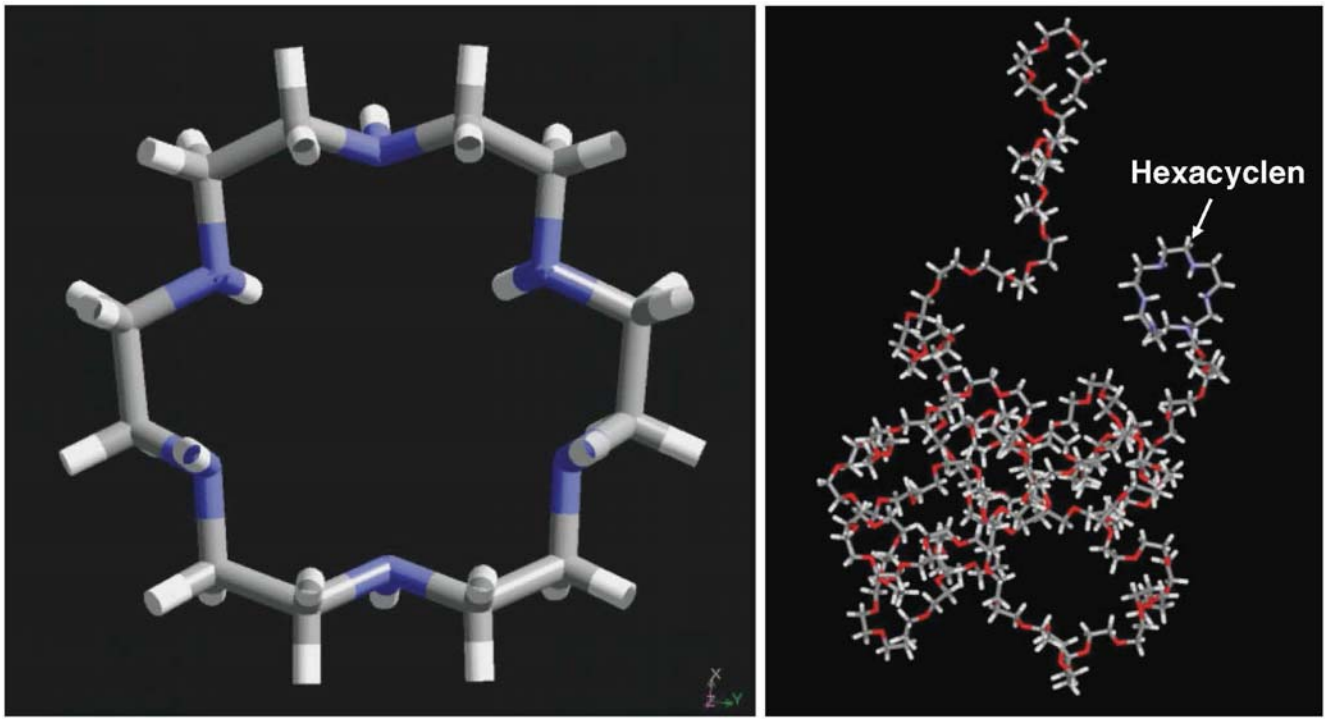

Scheme 1. Left: Structure of the 1,4,7,10,13,16-hexaazacyclooctadecan (hexacyclen) macrocycle. Right: The vacuum structure of PEG–*b*–hexacyclen made using the Cerius^2 software. Gray: carbon, white: hydrogen, blue: nitrogen, red: oxygen.

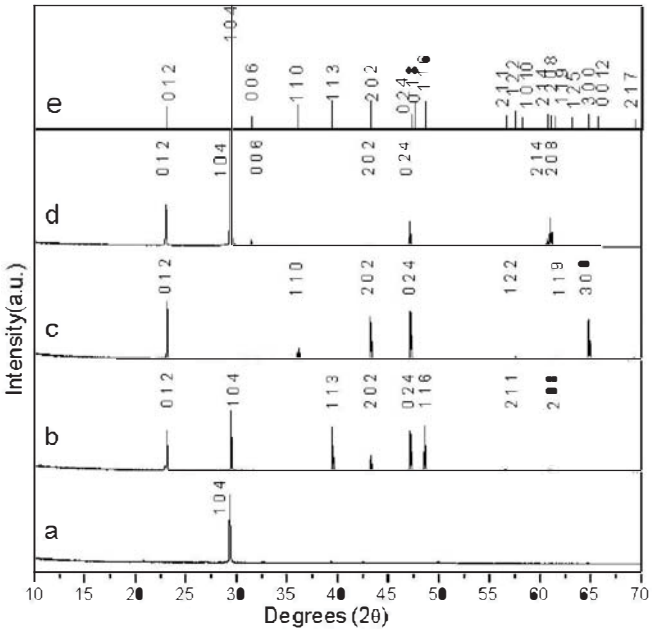

Figure 1. XRD patterns of $CaCO_3$ obtained after two weeks of gas-diffusion reaction: a) [polymer] = 0.2 g L^{-1}, [$CaCl_2$] = 10 mM, starting pH 4; b) [polymer] = 1 g L^{-1}, [$CaCl_2$] = 10 mM, starting pH 4; c) [polymer] = 2 g L^{-1}, [$CaCl_2$] = 10 mM, starting pH 4; d) [polymer] = 1 g L^{-1}, [$CaCl_2$] = 10 mM, starting pH 8; e) the standard diffraction pattern for calcite (Joint Committee on Powder Diffraction Standards (JCPDS) card no. 83-0578).

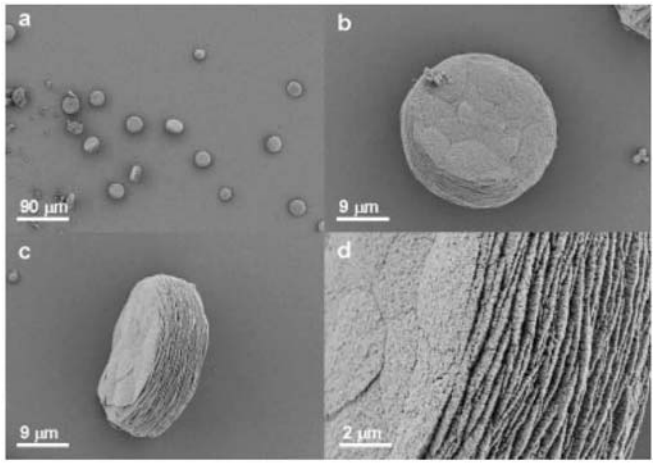

Figure 2. Typical SEM images of pancake-like self-stacked $CaCO_3$ obtained after two weeks of gas-diffusion reaction in the presence of 1 g L^{-1} PEG–*b*–hexacyclen, starting pH 4, [Ca^{2+}] = 10 mM: a) low-magnification image; b,c) face and lateral views, respectively, at high magnification; d) higher-magnification image of the specimen shown in (c).

shows that the thinner layers always originate from and overlap with their original thicker layers, and several pieces are formed from the center or the rims (Figs. 2b,c). The layer has a porous morphology, which has rarely been reported previously.[19] The detailed surface structures are shown in Figures 3a,b.

In a time-dependent study, the primary product after a 30 min reaction was an aggregate of amorphous particles (Fig. 4a), analogous to other $CaCO_3$ precursor structures.[20] The precipitate, after a 1 h reaction, was found to consist of

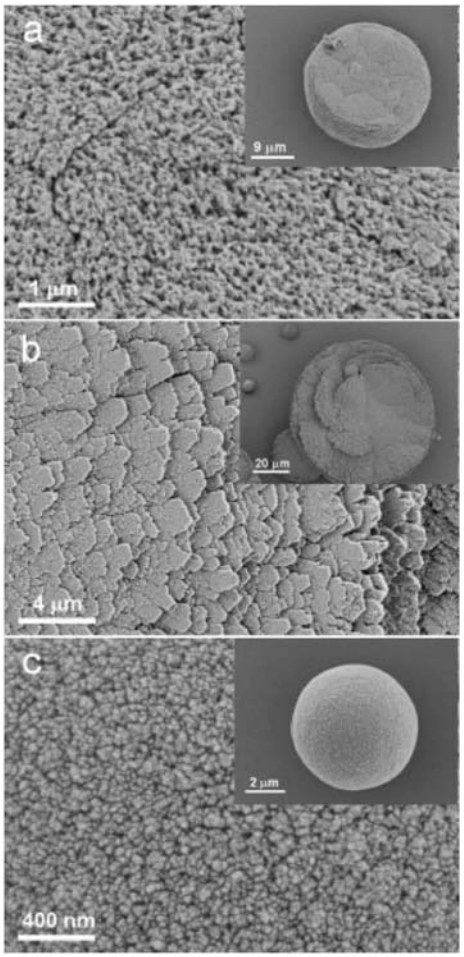

Figure 3. High-resolution SEM images of the surfaces of $CaCO_3$ pancakes obtained after the two-week gas-diffusion reaction (starting pH 4) showing the effect of different polymer concentrations, with $[Ca^{2+}] = 10$ mM: a) [polymer] = 1 g L^{-1}; b) [polymer] = 0.2 g L^{-1}. c) SEM image of the surface of a $CaCO_3$ spherule, [polymer] = 2 g L^{-1}.

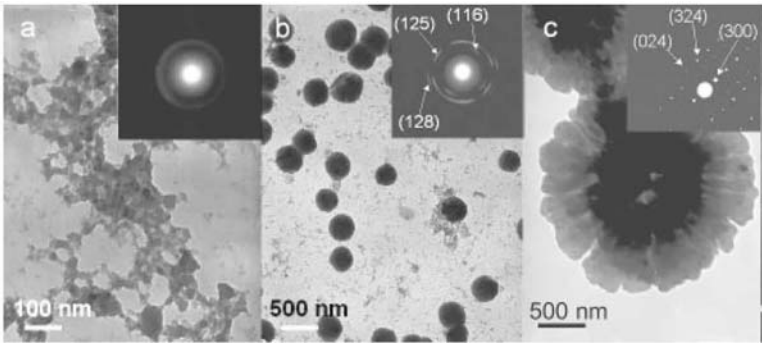

Figure 4. Transmission electron microscopy (TEM) images of the early formation stages of self-assembled $CaCO_3$ pancakes ([polymer] = 1 g L^{-1}, starting pH 4, $[Ca^{2+}] = 10$ mM). The corresponding reaction times are: a) 0.5 h, b) 1 h, and c) 3 days. The insets show selected area electron diffraction (SAED) patterns: a) amorphous, b) polycrystalline, and c) single crystal. The electron beam was projected along <02$\bar{1}$>.

monodisperse spheres with diameters of 300 nm (Fig. 4b). The SAED pattern already reveals the appearance of the first signs of crystallinity corresponding to a polycrystalline calcite phase, indicating a fast transformation from the amorphous to the crystallized calcite phase. After 3 h, the crystallinity increased (data not shown), and on increasing the reaction time from 3 h to 3 days, thin calcite sheets tended to grow out of the original mother crystals (Fig. 4c) to form round, self-stacked, $CaCO_3$ pancakes with diameters of 2.5 μm. It is remarkable that the SAED patterns in Figures 4b,c show unusual calcite faces that were not found in the wide-angle X-ray scattering (WAXS) pattern of the final crystal (see Fig. 1b), indicating that the view of the crystal was tilted in the SAED measurements (here, the <02$\bar{1}$> zone). This hindered face assignment in the early stages of crystal growth.

The polymer concentration had a significant effect on the structure of the crystals. When the polymer concentration decreased from 1 to 0.2 g L^{-1}, the pancake-like self-stacked morphology was retained, but the size distribution became rather inhomogeneous and the crystal size was larger than 60 μm (Fig. 3). The stacking of the pancake-like subunits was not as tight and thick as for a polymer concentration of 1 g L^{-1}, as observed in Figure 2. However, splaying of the outer layers was observed (Fig. 3b). Increasing the polymer concentration to 2 g L^{-1} led to the formation of spherical particles 6–8 μm in diameter, revealing the trend of smaller particle size with increasing polymer concentration (Fig. 3c). In addition, the particle surface became smoother and the crystallization time increased with increasing polymer concentration, because of the stabilization of smaller building blocks. An increase of only the Ca^{2+} concentration led to the formation of pancakes with rougher surface structures, as shown in Figure 5.

When the starting pH was increased to 8, only aggregates composed of film-like thin crystals with calcite structures were produced, indicating that a high pH value is not favorable for the self-assembly of complex pancakes because the NH groups are not protonated and the functional groups show weak interaction with the specific planes (see Supporting Information, Fig. 1). At pH 10, the polymer totally lost its ability to control the particle morphology.

The surface of the crystals became rougher when the polymer concentration decreased from 1 to 0.2 g L^{-1} (starting pH 4, Fig. 3). The XRD pattern in Figure 1a almost exclusively shows (104) diffraction, implying that this plane was parallel to the substrate and was the only exposed plane. The epitaxial match of the hexacyclen onto (104) was not as perfect as that to the (001) face; thus, from the epitaxial viewpoint, (001) should be exposed, which was not observed for any sample (see Supporting Information, Fig. 2). However, the (104) plane exposes surface cations and anions, obviously leading to tighter polymer binding by additional complexing of Ca^{2+}. These findings already

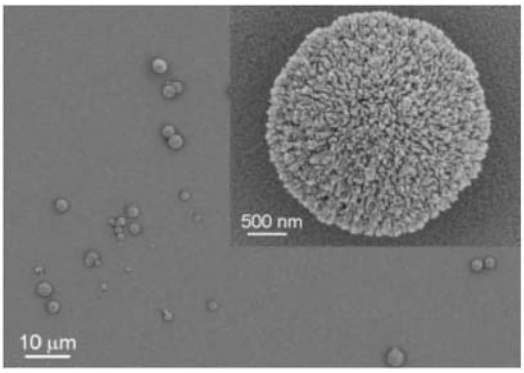

Figure 5. SEM image of the calcite disks with rough surfaces obtained by the two-week gas-diffusion reaction; the starting pH was 4, [polymer] = 1 g L^{-1}, [Ca^{2+}] = 20 mM. The inset shows a magnified image of one of the disks.

indicate that preferred polymer binding to (1●4) cannot be solely due to an epitaxial match.

At a polymer concentration of 1 g L^{-1} (pH 4), additional faces like (●12/●24), (113), (116), and (2●2) were detected by WAXS (Fig. 1) as (1●4) appeared to be fully occupied by the polymer. None of these faces has a good epitaxial match to the adsorbed hexacyclen (see Supporting Information, Fig. 3). (2●2) at least seems to geometrically match the polymer, whereas (●12) has a reasonable match, combined with a high surface-ion density. Thus it is understandable that, at a polymer concentration of 2 g L^{-1} with a still longer crystallization time, the polymers can rearrange to good binding faces so that (113) and (116) are not found anymore, but (●12) becomes a strong peak. Interestingly, (1●4) is not exposed at all and instead (3●●) is found, which also has surface cations and anions but should be less favorable than (1●4). The reason for this is not yet clear. Therefore, the simple epitaxial model, as often stressed in the discussion of biomineralization mechanisms, cannot explain our findings as, otherwise, only (●●1) faces should be formed. Instead, it is a complicated counter play between particle stabilization, epitaxial match, crystallization time, and thus time for polymer rearrangement, and surface-ion density that determines the polymer adsorption on exposed faces, and thus the final particle morphology. Previously, Weiner and Traub proposed an epitaxial model for aragonite nucleation in nacre.[12,13] However, a recent report by Volkmer et al. also demonstrated that it is not the epitaxial match, but the charge density, which plays a key role in the oriented growth of $CaCO_3$ crystals under a monolayer of amphiphilic octaacids,[21] which may be consistent with our present findings on the interaction of a soluble polymer with $CaCO_3$ crystals. However, we have to stress that none of these mechanisms can exclusively explain the case investigated here, wherein the possibility of free, face-selective polymer adsorption in three dimensions exists. In fact, counter play between these mechanisms as well as additional factors has to be considered.

The shape-evolution process for the formation of $CaCO_3$ pancakes reported above suggests that the growth process involves the following steps: i) Amorphous nanoparticles stabilized by the polymer form at the early stage; ii) The calcite phase is formed by phase transformation, or more likely by dissolution–recrystallization, and then the crystals grow by directed aggregation under control of the polymer, similar to the recently reported so-called "mesocrystals".[22,23] As soon as the crystalline material forms, the polymer starts selectively adsorbing onto the negative crystal faces, and this leads to gluing together of the flakes formed. When the polymer concentration is low, net repulsion is still evident, leading to a splaying out of the pancakes at a concentration of 1 g L^{-1}, but the pancakes are more or less still glued together. At a concentration of 2 g L^{-1}, even the smallest flakes formed are immediately glued together, resulting in the minimum energy morphology, the sphere, for which the gluing of the primary units should be at a maximum. iii) Newly formed layers nucleate from the mother layer by an epitaxial growth mode. The fast double-jet reaction in the presence of the same polymer using Na_2CO_3 as the carbonate source, instead of the slow gas-diffusion process, can only generate thinner pancakes without multilayers (Fig. 6), indicating that the slow gas-diffusion reaction with the associated pH increase is favorable for the epitaxial growth of multilayered pancakes. iv) The nucleation on the mother layer is projected out, and forms new layers in a stepwise manner.

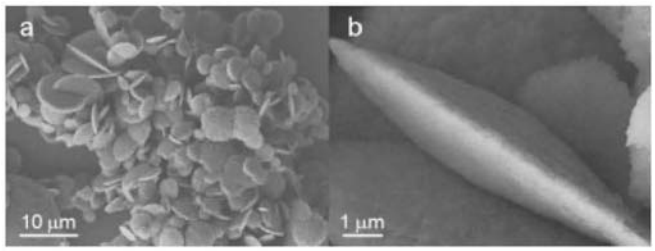

Figure 6. SEM images of the calcite disks obtained by the double-jet technique after reaction and aging for one week, starting pH 4. a) Low-magnification image and b) high-magnification image of a typical disk.

In conclusion, a PEG–*b*–hexacyclen macrocycle can be used as a modifier for the controlled self-assembly of complex and unusual calcite pancakes with multiple stacked layers. The shape and surface structure can be controlled by adjusting the polymer concentration, the initial pH value, as well as the concentration of calcium ions, demonstrating that it is not only epitaxial match that drives selective polymer adsorption, but also charge/ion surface density, particle stabilization, and the time for polymer rearrangement (from initially occupied less-favorable faces to more-preferred faces). Such rearrangement of polymers to favorable faces can be understood as a sort of curing mechanism, which is likely enhanced by the block copolymer character with a second soluble but non-in-

teracting block. The results demonstrate that it is possible to manipulate the ability of selective adsorption and stabilization of the DHBCs in order to control the directed crystal growth process, in agreement with computer visualization of the polymer–crystal interaction. The synthetic method is simple, mild, and controllable, and provides a convenient route to synthesize hierarchical nanostructures based on a polymer-directed crystallization mechanism, even in a predictable manner.

Experimental

All chemicals were of analytical grade and used as received without further purification. In a synthesis similar to that described by Addadi and co-workers, the polymer was added to a calcium chloride solution, into which carbonate was introduced via vapor diffusion [18]. All the glassware (glass bottle and small pieces of glass substrates) was cleaned and sonicated in ethanol for 5 min, rinsed with distilled water (18 $\Omega M cm^{-1}$), further soaked in a H_2O/HNO_3 (65 %)/H_2O_2 (1:1:1, v/v/v) solution, rinsed with doubly distilled H_2O, and finally dried with acetone.

The mineralization of $CaCO_3$ was carried out in a glass bottle with a volume of 15 mL, which was put into a closed dessicator at room temperature (25 °C). A stock aqueous solution of $CaCl_2$ (0.1 M) was freshly prepared in boiled doubly distilled water and bubbled with N_2 overnight before use. In a typical procedure, 500 μL of a 0.1 M $CaCl_2$ solution was injected into 5 mL 1 $g L^{-1}$ polymer solution under mild stirring. The pH was adjusted to a fixed value using dilute HCl or NaOH. Then, three glass substrates were carefully placed at the bottom of the bottle to collect the crystals. The bottles were then covered with parafilm, which was punched with 3 needle holes, and placed in a larger dessicator. Two small glass bottles (10 mL) of crushed ammonium carbonate were also covered with parafilm, punched with 3 needle holes, and placed at the bottom of the dessicator. After different periods of time, the parafilm was removed and the precipitate was rinsed with distilled water and ethanol, and allowed to dry at room temperature. The time-dependent crystallization experiments were done by taking out the glass substrates from the bottles, in order to stop the reaction for examination. The precipitates were collected and washed with distilled water and dried in air for further characterization.

The double-jet experiments were carried out in a thermostated vessel (25 °C). 5 mL distilled water (pH 5.6) was placed in the vessel. Then, solution A and solution B (solution A: 5 mL of 30 mM $CaCl_2$ containing 3 $g L^{-1}$ polymer, pH 1; solution B: 5 mL of 30 mM Na_2CO_3, pH 10.6) were injected into the vessel containing 5 mL water at a rate of 0.5 mL min^{-1} under mild stirring. [Ca^{2+}] in the final solution, which was equal to [CO_3^{2-}], was 10 mM, with a polymer concentration of 1 $g L^{-1}$ and an adjusted pH value of 4. After complete injection, the solution was aged for 3–4 days. Then, the crystals were collected for characterization.

The small pieces of cover slips and the crystals were examined by optical microscopy, and then they were coated with gold for scanning electron microscopy (SEM) measurements on a DSM 940A (Carl Zeiss, Jena) microscope. Powder X-ray diffraction (XRD) patterns were recorded on a PDS 120 diffractometer (Nonius GmbH, Solingen) with Cu Kα radiation. The surface cleavage of the crystal faces and the cell structure were performed with the aid of the Cerius^2 software (Accelrys).

[1] J. R. Young, S. A. Davis, P. R. Bown, S. Mann, *J. Struct. Biol.* **1999**, *126*, 195.

[2] a) H. A. Lowenstam, S. Weiner, *On Biomineralization*, Oxford University Press, Oxford **1989**. b) S. Mann, *Biomineralization—Principles and Concepts in Bioinorganic Materials Chemistry*, Oxford University Press, Oxford **2001**.

[3] a) S. Mann, *Angew. Chem. Int. Ed.* **2000**, *39*, 3392. b) G. A. Ozin, *Acc. Chem. Res.* **1997**, *30*, 17. c) S. W. Weiner, L. Addadi, *J. Mater. Chem.* **1997**, *7*, 689. d) L. A. Estroff, A. D. Hamilton, *Chem. Mater.* **2001**, *13*, 3227. e) T. Kato, A. Sugawara, N. Hosoda, *Adv. Mater.* **2002**, *14*, 869. f) H. Cölfen, S. Mann, *Angew. Chem. Int. Ed.* **2003**, *42*, 2350. g) F. C. Meldrum, *Int. Mater. Rev.* **2003**, *48*, 187. h) S. H. Yu, H. Cölfen, *J. Mater. Chem.* **2004**, *14*, 2123.

[4] a) R. Kniep, S. Busch, *Angew. Chem. Int. Ed.* **1996**, *35*, 2624. b) S. Busch, H. Dolhaine, A. DuChesne, S. Heinz, O. Hochrein, F. Laeri, O. Podebrad, U. Vietze, T. Weiland, R. Kniep, *Eur. J. Inorg. Chem.* **1999**, *10*, 1643.

[5] a) Z. R. Tian, J. A. Voigt, J. Liu, B. Mckenzie, M. J. Mcdermott, *J. Am. Chem. Soc.* **2002**, *124*, 12954. b) Z. R. Tian, J. A. Voigt, J. Liu, B. Mckenzie, M. J. Mcdermott, M. A. Rodriguez, H. Konishi, H. F. Xu, *Nat. Mater.* **2003**, *2*, 821.

[6] a) A. Taubert, C. Kubel, D. C. Martin, *J. Phys. Chem.* **2003**, *107*, 2660. b) A. Taubert, D. Palms, G. Glasser, *Langmuir* **2002**, *18*, 4488.

[7] S. H. Yu, H. Cölfen, K. Tauer, M. Antonietti, *Nat. Mater.* **2005**, *4*, 51.

[8] Z. Y. Tang, N. A. Kotov, S. Magonov, B. Ozturk, *Nat. Mater.* **2003**, *2*, 413.

[9] a) A. P. Jackson, J. F. V. Vincent, R. M. Turner, *Proc. R. Soc. London, Ser. B* **1988**, *234*, 415. b) A. M. Belcher, X. H. Wu, R. J. Christensen, P. K. Hansma, G. D. Stucky, D. E. Morse, *Nature* **1996**, *381*, 56.

[10] E. Dalas, P. Klepetsanis, P. G. Koutsoukos, *Langmuir* **1999**, *15*, 8322.

[11] H. Cölfen, *Curr. Opin. Colloid Interface Sci.* **2003**, *8*, 23.

[12] S. Weiner, W. Traub, *FEBS Lett.* **1980**, *111*, 311.

[13] S. Weiner, *Phil. Trans. R. Soc. London, Ser. B* **1984**, *304*, 425.

[14] B. R. Heywood, in *Biomimetic Materials Chemistry* (Ed: S. Mann), Wiley-VCH, Weinheim, Germany **1996**.

[15] H. Cölfen, *Macromol. Rapid Commun.* **2001**, *22*, 219.

[16] R. M. Izatt, K. Pawlak, J. S. Bradshaw, *Chem. Rev.* **1991**, *91*, 1721.

[17] M. Sedlak, H. Cölfen, *Macromol. Chem. Phys., Suppl.* **2001**, *202*, 587.

[18] S. Weiner, S. Albeck, L. Addadi, *Chem. Eur. J.* **1996**, *2*, 278.

[19] J. Zhan, H. P. Lin, C. Y. Mou, *Adv. Mater.* **2003**, *15*, 621.

[20] H. Cölfen, L. M. Qi, *Chem. Eur. J.* **2001**, *7*, 106.

[21] D. Volkmer, M. Fricke, C. Agena, J. Mattay, *J. Mater. Chem.* **2004**, *14*, 2249.

[22] S. Wohlrab, N. Pinna, M. Antonietti, H. Cölfen, *Chem. Eur. J.* **2005**, *11*, 2903.

[23] T. X. Wang, H. Cölfen, M. Antonietti, *J. Am. Chem. Soc.* **2005**, *127*, 3246.